Elastic Electron Scattering by Laser-Excited $^{138}Ba(...6s6p\,^1P_1)$ Atoms

S. Trajmar[†], I. Kanik[†], M. A. Khakoo[‡], L. R, LeClair[†0], 1. Bray*, D. Fursa* and G. Csanak[x]

[†] California Institute of Technology, Jet Propulsion Laboratory, Pasadena, CA 91109

[‡] California State University, Department of Physics, Fullerton, CA 92634

[*] Electronic Structure of Materials Centre, The Flinders University of South Australia, G.P. O. Box 2100, Adelaide 5001, Australia

[x] University of California, Los Alamos National Laboratory, Los Alamos, NM 87544

[0] Present address: MPB Technologies, Pointe Claire, Quebec H9R 1E9, Canada

PACS number(s): 34.80.Qb, 34.80.Dp

To be submitted to

Physical Review Letters

APRIL 17, 1997

Abstract

The results of a joint experimental and theoretical study concerning elastic electron scattering by laser-excited ^{138}Ba (...$6s6p\ ^1P_1$) atoms are presented. From these studies, we extracted differential scattering cross sections (DCS's) and collision parameters for elastic scattering by the coherently prepared $^1P_1$ atoms. We also obtained from our experimental results DCS's and electron-impact coherence parameters (EICP's) for elastic scattering by atoms which were initially in the isotropic, incoherent $^1P_1$ level. Good agreement was found between the experimental results and those obtained from the convergent close-coupling (CCC) calculations. It was demonstrated that elastic scattering creates alignment with significant probability. As a by-product of our measurements, we also obtained DCS'S for elastic scattering by metastable ^{138}Ba atoms.

Electron scattering experiments on laser-excited atoms have been restricted mainly to superelastic scattering and their interpretation in terms of electron-impact coherence parameters (EICP's) for the inverse inelastic collision processes (see e.g. ref. [1]). Very few inelastic studies of this type have been carried out and no elastic scattering measurements have been reported so far for the purpose of extracting EICP's.

We describe here measurements concerning elastic electron scattering by ^{138}Ba (.. .6s6p $^1P_1$) atoms which were coherently excited by a linearly polarized laser beam. These measurements allowed us to extract various elastic differential cross sections (DCS's), EICP's and collision parameters for elastic scattering. In a parallel theoretical effort, we used the convergent close-coupling (CCC) approximation, along with the LS-coupling scheme, to calculate the magnetic-sublevel elastic scattering amplitudes for the Ba (^1P) atoms. From these amplitudes all the cross sections and parameters derived from the experiments have been obtained. Measurements were carried out at the electron impact energy (E_o) of 20.0 eV and scattering angles (θ) of 10°, 150, and 20° .Calculations were performed at the same energy over the 0° to 1800 angular range. These efforts were motivated by the question raised in connection with plasma polarization spectroscopy whether elastic electron scattering can create alignment and to what degree [2-5] and by the lack of experimental and theoretical data and insight concerning elastic electron scattering by excited atoms.

The experimental arrangement and measurement procedures can be briefly summarized as follows. A nearly monoenergetic (A $E_{1/2} \approx 0.08$ eV) and well-collimated beam of electrons intersected a collimated (aspect ratio = 1:10) Ba beam (naturally occurring isotopic mixture) at right angle. The Ba beam was illuminated by a laser beam which was either in the scattering plane or displaced by about 4 mm parallel to the scattering plane upstream the Ba beam. We refer to these laser positions as laser-C and laser-L positions, respectively. The laser beam (power ≈ 70 mW) was generated by a ring laser, operating in single mode, and was linearly polarized. The incident laser beam polar angles with respect to the electron collision frame were θ_v = 450 or 90° and ϕ_v = 0° or 180° for the present measurement. The z-axis of the collision frame was taken along the momentum of the incident electron. (See ref. [1] for more details.) The linear polarization angle (ψ), with respect to the scattering plane, could be continuously varied by rotating a half-wave plate. The laser wavelength was tuned to excite the 138 isotope of Ba (≈ 7 1.7°/0 of the isotopic mixture) from the ground state to the . .6s6p $^1P_1$ state. The scattered electrons were detected over a small solid angle (≈ 10^{-3} steradian). The detector could be rotated around the axis of the Ba beam in the -750 to +600 angular range with respect to the incoming electron beam. The detected electrons were counted as a function of various parameters (E_0, 0, ψ, energy loss etc.) using a computer-controlled multichannel-scaler.

The measured count rates (I_{TOT}) in the elastic scattering experiment, for the laser-C position include contributions from background (I_B), from elastic scattering by ground state atoms of all isotopes (I_G^{el}) and from elastic scattering by coherently excited $^1P_1$ (I_{cP}^{el}) and cascade populated $^3D_2$ and $^1D_2$, metastable (I_m^{el}) ^{138}Ba atoms. In the case of the laser-L position, the $^1P_1$ species decay by radiation to the ^{1}SO ground state and to the $^1D_2$ and $^3D_2$ metastable levels by the time they reach the collision region. In order to separate I_{cP}^{el} from other contributions, to achieve the conversion of this signal to absolute cross sections, and to be able to extract EICP's and collision parameters from the experiments, we needed to carry out 116 measurements of various kinds for each fixed E_0, θ case. These measurements involved the inelastic ($^1SO \rightarrow {}^1P_1$), the superelastic ($^1P_1 \rightarrow$ lS.) and the elastic channels. Scattering intensities for various combinations of Ba beam turned ON and OFF, laser beam turned ON and OFF (for both laser-C and laser-L positions) and for four laser geometries (O_v = 450 and 90° both with ϕ_v = 0° and 180°) as well as the modulation of the elastic and superelastic scattering intensities as a function of ψ *were* measured. In addition, the laser-induced-fluorescence signal (for ψ = 90°) was continuously monitored. Normalization of the $I_{cP}^{el}(\psi)$ signal to the corresponding differential cross section, $DCS_{cP}^{el}(\psi)$, was achieved by measuring the ratios of this elastic scattering signal to the signal associated with the ($^1S_o \rightarrow {}^1P_0$) inelastic scattering and utilizing the derived population fractions and the ($^1S_o \rightarrow {}^1P_0$) inelastic DCS values of Wang et al. [6].

At this stage, we have (for a fixed E_0, O case) a modulation equation of the type

$$DCS_{cP}^{el}(\psi) = A^{Exp} + B^{Exp}\cos 2\psi = \tfrac{3}{4}\, DCS_{P}^{el}\,\{A + B\cos 2\psi\} \qquad (1)$$

for each laser geometry [1]. The values of A^{Exp} and B^{Exp} were obtained from least squares fitting of the experimental data. We denote here, and in the following discussions, the DCS's associated with scattering processes where the initial atomic states are prepared by coherent excitation to the $^1P_1$ state with a particular laser geometry and polarization as $DCS_{cP}(\psi)$. For DCS's associated with processes where the initial and/or final magnetic sublevel is specified (or averaged over incoherently), we use the notation $DCS_P^{el}(M_i, M_f)$, $DCS_P^{el}(M_i = M)$, $DCS_P^{el}(M_f = M)$ and DCS_P^{el} and omission of M_i and/or M_f implies averaging (summation) over those magnetic sublevel quantum numbers. M can take the values of- 1, 0 or +1. Since the spin of the scattering electrons was not selected or detected in the present measurements, averaging over initial and summation over final spin quantum numbers are always assumed.

The modulation equations (eqn.1) can be used in two different ways: (i) to obtain from them EICP'S and DCS's for the inverse process: elastic scattering by an isotropic, incoherent ensemble of ^{138}Ba (. .6s6p $^1P_1$) atoms, (ii) to obtain from them collision parameters and DCS'S for elastic scattering by a coherent (unisotropic or isotropic) ensemble of ^{138}Ba (.. .6s6p $^1P_1$) atoms.

For evaluation of the modulation equations in terms of the "inverse" process we have for the modulation coefficients [1]:

$$A = 1 + \cos^2\theta_n + (\lambda - 1)\cos\varepsilon\,\sin^2\theta_n + \kappa\sin 2\theta_n\cos\phi_n \qquad (2a)$$

$$B = (3L - 1)\sin^2\theta_2 + (1 - \lambda)\cos\epsilon(1 + \cos^2\theta_n) + \kappa \sin 2\theta_n \cos\phi_n , \quad \text{(2b)}$$

where

$$\kappa = 2\sqrt{\lambda(1 - \lambda)}\cos\chi = 2\sqrt{\lambda(1 - \lambda)}\cos\Delta\cos\tilde{\chi} . \quad \text{(2C)}$$

In the present experiments, $\theta_n = \theta_v + \theta\cos\phi_v$ and for scattering to the left we have $\phi_n = \phi_v = 0°$ and for scattering to the right we have $\phi_n = \phi_v = 180°$. The modulation equations involve the four EICP's *(A, cos* ϵ, *cos* A and $\tilde{\chi}$) as defined by Paixao et al. [7] and applied to the Ba superelastic scattering by Zetner et al. [1]. From our laser-in-plane measurements we can extract only λ, cos ϵ and κ. These EICP's can be obtained by solving any set of three equations defining A or B for laser geometries involving $\theta_v = 45°$, $\phi_v = 0°$ and 180° and $\theta_v = 90°$, $\phi_v = 0°$ or 180°. (We used the two θ_v = 90" modulation data to check left/right scattering symmetry and then took their average as the third modulation equation.) There are 16 meaningful such combinations, each yielding a set of EICP's. We took the average of these 16 sets as our experimental values. Definition of these EICP's for a ($^1S_0 \leftrightarrow$ 'P_1) process is given by Zetner et al. [1]. The only difference here is the generalization from the ($^1S_0 \leftrightarrow {}^1P_1$) to the ($^1P_1 \leftrightarrow {}^1P_1$) transition which requires averaging over the initial magnetic sublevels of the $^1P_1$ level. From *A* and DCS, we obtained DCS(M_f = O). From DCS (M_f = O) and DCS, the DCS (M_f = 1) values were calculated. (Determination of the DCS will be described below.)

For the evaluation of the modulation equations in terms of the actual experimental process, we used equations of the same form as 2a, b and c except A, cos ϵ, κ, cos A and cos $\tilde{\chi}$ were replaced by p_1, p_2, h, p_3 and p_4, respectively and 0, = θ_n. These equations are formally similar to eqns. (2a, b and c) and can be derived in a straightforward manner [8-9]. The collision parameters, p_1, p_2 and *h* were obtained from a procedure similar to that described above for the EICP's. These parameters relate to the actual experimental process as described above under (ii). They are useful, in the sense that they allow us to calculate the $DCS_{cP}^{el}(\psi)$ value associated with *any initial state* prepared by in-plane laser excitation of arbitrary geometry and linear polarization. The azimuthal asymmetry (A) of elastic scattering is defined as the difference in the left and right scattering intensities (or equivalent cross sections) divided by the sum of the two. This asymmetry is the consequence of the polarized nature of the initial atomic state and it appears for laser geometries other than $\theta_v = 90°$.

For certain laser geometries and polarizations $DCS_{cP}^{el}(\psi)$ is simply equal to $DCS_P^{el}(M_i = O)$, $DCS_P^{el}(M_i = 1)$ or $DCS_P^{el}(M_i$ = isotropic and coherent) which is associated with elastic scattering by atoms initially in a coherent, isotropic state. We also have

$$DCS_{cP}^{el}(\psi_m)^+ + DCS_{cP}^{el}(\psi_m)^- = 2\ DCS_P^{el} \tag{3a}$$

and

$$DCS_{cP}^{el}(\psi_m)^+ - DCS_{cP}^{el}(\psi_m)^- = 2\ h\ DCS_P^{el}, \tag{3b}$$

where ψ_m is the "magic" polarization angle satisfying the condition $\cos 2\psi_m = ⅓$ and the +(-) sign refers to ϕ_v = 00(1 800). Eqn. (3a) was used to get the values of DCS_P^{el}.

The calculations have been performed combining the LS-coupling CCC method for helium [10] and the one for quasi one-electron targets [11]. The Ba atom is treated as two active electrons have a fixed Hartree-Fock with wave-polarization potential core. Details of the calculation will be given elsewhere.

It is interesting to note that in the present experiments the modulation of the elastic scattering signal (as given by eqn. 1) was found to be 90° out of phase with that of the superelastic signal. (While ψ = O yields maximum for the ($^1P_1 \rightarrow$ lS.) scattering, it yields minimum for the ($^1P_1$ - $^1P_1$) scattering.)

Selected values of a large set of the measured and calculated cross sections and the EICP's are shown over the full angular range in Figs. 1 and 2, respectively. The estimated experimental error limits for these quantities are *30'%.* for the differential cross sections and for the λ and p_1 parameters and 40°/0 for the cos ϵ and p_2 parameters. The *h* and *k* parameters can not be reliably extracted from the present measurements. This is due to the fact that these parameters are small compared to the errors associated with the modulation coefficients and to the nature of error propagation. A reliable extraction of these parameters would require the knowledge of these modulation coefficients to within a few percent.

In Fig. 1 three theoretical DCS's are shown *over* the full angular range and compared to the experimental results. The experimental and theoretical results agree well within the estimated error limits. The values for these cross sections drop almost five orders of magnitude between 0° and 70°. A shoulder with an inflexion point at around 35° and two deep minima at around 72° and 134° appear in the theoretical curves. The same general behavior is found for the other DCS_P^{cl} (M_i = M) and DCS_P^{cl} (M_f = M) curves. They not only show the same shape, in general, but also have the same order of magnitude values, except for the DCS_P^{cl} (M_f = M) curves which are multiplied by the factor of $1/(2J_i + 1) = 1/3$ coming from the averaging over M_i. The DCS_{cP}^{cl} (M_i = cob. ± 1) curve shows deeper and sharper minima than the others. (M_i = cob. + 1 refers to an initial state which is a coherent superposition of the +1 and -1 magnetic sublevels). These observations indicate weak dependence on M_i and h&for DCS_P^{cl} (M_i = M) and DCS_P^{cl} (M_f = M), respectively. The calculations show that the various DC $S_P^{el}(M_i, M_f)$ values differ by more than an order of magnitude but these differences are washed out, to a large extent, in the averaging processes. The difference in $DCS_P^{el}(M_i = 1)$ and $DCS_P^{el}(M_i = O)$ values, which determines the alignment creation cross section, is significant at most scattering angles. These differences, expressed in percent with respect to the DC $S_P^{el}(M_i = O)$ values, are about 30% at low angles, decrease to O% around 0 = 70° and increase to around 300% at high angles. It is clear from the present study that measurement of the cross sections at high scattering angles would be extremely difficult and one will have to rely on theoretical calculations in these regions.

In Fig. 2 the EICP's, λ and cos ϵ are shown. Not surprisingly, very good agreement between experiment and theory is found for λ since it represents the ratio oft wo cross sections which both show, separately, good agreement between experiment and theory. Somewhat less satisfactory is the agreement for cos ϵ. While no significant features appear in the A curve, the cos ϵ curve shows a deep minimum at around 22° and two sharp maxima at around 72° and 1350. Two steep maxima in cos ϵ are caused by the deep minima in the DCS curve (Kessler effect) since the EICP's are normalized by DCS's. The deviation of cos ϵ from the value of unity for the theoretical curve is strictly due to the averaging over M_i which causes the loss of coherence between the $M_f = 1$ and $M_f = -1$ scattering amplitudes. For the experimental value, some loss-of-coherence may also be due to spin-orbit coupling effects and this may account to some extent to the less satisfactory agreement between experiment and theory.

The angular behavior of the collision parameters p_1 and p_2 are very similar to those of λ and cos ϵ, respectively. The agreement between theory and experiment can also be similarly characterized. The azimuthal asymmetry for elastic scattering is available only from theory. For the $\theta_v = 450$ and $\psi = 0°$ laser arrangements, we have the maximum value for A. The present calculations predict, under these conditions, A_{max} values of 0.032, 0.154 and 0.290 for θ = 10°, 150 and 20°, respectively at E_0 = 20 eV.

The fully averaged DCS_P^{el} values derived from the present work are associated with elastic scattering by ^{138}Ba ($^1P_1$, isotropic, *incoherent)* atoms, It is interesting to compare these DCS's with those obtained for ^{138}Ba ($^1P_1$, isotropic, ***coherent***) atoms to see how much effect the coherence among the magnetic sublevels for the initial state makes. An isotropic (and coherent) initial state is prepared by laser excitation when the laser geometry is θ_v =45 and ϕ_v = O or 180° and $\psi = \psi_{magic}$ (based on the population equations given by Li and Zetner [9]). For these conditions, we have the two cross sections $[DCS_{cP}^{el}(\psi_{magic})^{\pm}]$ which differ from DCS_P^{el} by $\pm h$, respectively. Again, the observation of this coherence effect is not possible in the present experiments.

Considering the complexity of the experiments and the fact that the theoretical calculations neglect spin-orbit coupling effects, the general agreement between theory and experiment is surprisingly good for the E_0 = *20* eV, θ = 10°, 150, 20° cases. This agreement indicates that spin-orbit coupling effects as well as extended scattering volume effects (see ref. [1]) are not dominant here. One can, therefore, rely on theory to obtain the integral elastic and alignment creation $[Q^{[2]}_{CR}]$ cross sections. Table I summarizes these results. The alignment creation cross section for elastic scattering is about an order of magnitude smaller than the other integral elastic scattering cross sections but by no means is it negligible and this answers the question raised above concerning alignment creation by elastic electron collisions.

As a by-product of our measurements, we also obtained differential elastic scattering cross sections for metastable ^{138}Ba atoms *(57.8* 17.3, 17.9* ± *5.4* and 7.1 ± *2.1 x* 10^{-16} cm^2/sr at 10°, 15°, and 20°, respectively). The measurements yielding these cross sections were necessary to determine the metastable population fractions in the target region for the laser-L and laser-C positions. The signal associated with elastic scattering by metastable atoms showed no modulation with ψ indicating that the cascade process populating these levels resulted in the same (isotropic) magnetic sublevel distribution in these levels for any alignment of the initial $^1P_1$ level. Reconsider, therefore, the experimental values to correspond to full averaging over magnetic sublevels (and continuum electron spins). Based on the branching ratio determined by Bizzari and Huber [12] for the ($^1P_1$ - $^1D_2$) and ($^1P_1 \rightarrow {}^3D_2$) decays, we have $DCS^{el}_m = 0.7\ DCS^{el}(^1D_2) + 0.3\ DCS^{el}(^3D_2)$.

The present study demonstrates the feasibility of extracting magnetic sublevel specific differential elastic scattering cross sections, collision parameters and information concerning the creation of alignment by elastic scattering from measurements involving laser-excited atoms. These measurements are, however, time consuming and difficult and can not be expected to supply a large database but only to serve as benchmark for checking calculational schemes which could then generate the full set of data required for various purposes. The present CCC method seems promising for this purpose but inclusion of spin-orbit effects is desirable.

Acknowledgments

The experimental part of this work was carried out at the Jet Propulsion Laboratory, California Institute of Technology. The authors acknowledge the financial support by NSF, NASA, NRC and DOE. We wish to express our gratitude to Professors T. Fujimoto and S. A. Kazantsev for calling our attention to the question of alignment creation in elastic scattering and for valuable discussions. We also acknowledge the support of the South Australian Centre for High Performance Computing and Communications.

References

[1] P. W. Zetner, S. Trajmar and G. Csanak, Phys. Rev A **41, 5980 (1990).**

[2] T. Fujimoto, private communication (1 996).

[3] S. A. Kazantsev, private communication (1996).

[4] A. G. Petrashen, V. N. Rebane and T. K. Rebane, Opt. Spectrosec. (USSR) S5, 492 (1984).

[5] E. I. Dashevskaya and E. E. Nikitin, Sov. J. Chem. Phys. 4, 1934 (1987).

[6] S. Wang, S. Trajmar and P. W. Zetner, J. Phys. B. 271613 (1 994).

[7] F. J. da Paixão, N. T. Padial, G. Csanak and K. Blum, Phys. Rev. L 45, 1164 (1 980).

[8] P. W. Zetner (private communication, 1994).

[9] Y. Li and P. W. Zetner, J. Phys. B 29, 1803 (1 996).

[10] D. V. Fursa and 1. Bray, Phys. Rev. A 52, 1279 (1995).

[11] I. Bray, Phys. Rev. A 49,1066(1994).

[12] A. Bizzari and M. C. E. Huber, **Phys. Rev. A 42,5422 (1990).**

Table I. Summary of the calculated integral elastic and alignment creation cross sections at $E_0 = 20$ **eV** (10-16 cm^2 units).

$Q\ (M_f = 0)$	9.56
$Q\ (M_f = 1)$	12.52
$Q\ (M_i = 0)$	28.42
$Q\ (M_i = 1)$	37.71
$Q\ (M_i =$ cob. $\pm 1)$	42.21
Q	34.61
$Q^{[2]}_{CR} = (2/3)^{\%} [Q\ (M_f = 1) - Q\ (M_f = 0)]$	2.42

Figure Captions

1. Elastic differential electron scattering cross sections for $^{138}Ba\,(^1P_1)$ atoms at $E_0 = 20$ eV. Lines represent the results of CCC calculations. The corresponding experimental values are indicated by symbols. Experimental error limits are also shown.

2. The EICP's (λ and cos ϵ) for elastic electron scattering by $^{138}Ba\,(^1P_1)$ atoms at $E_0 = 20$ eV. ● indicates the present experimental results with error limits, the lines are from the present CCC calculations.

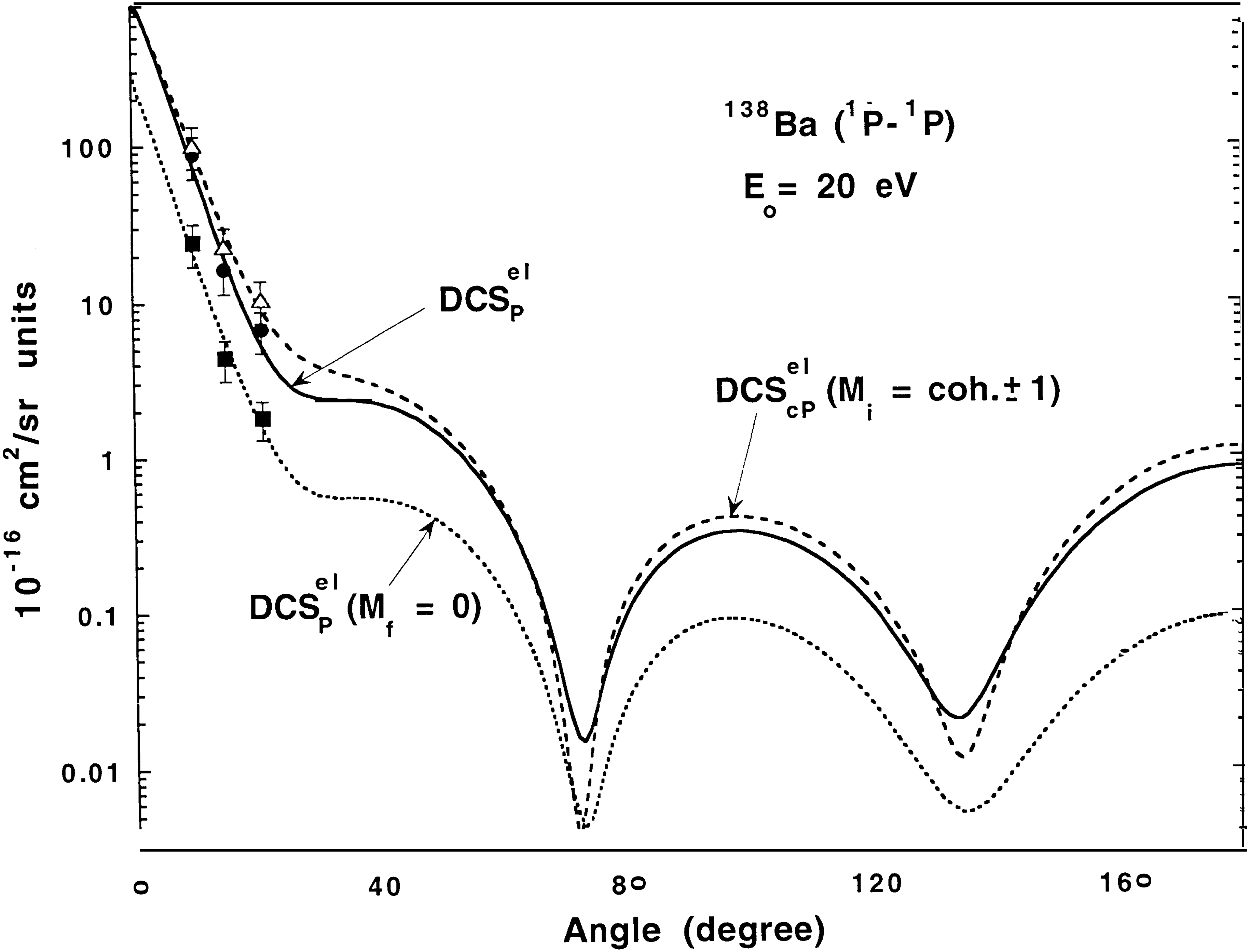

^{138}Ba (^{1}P-^{1}P)
E_o = 20 eV
DCS_P^{el}
DCS_{cP}^{el} (M_i = coh.±1)
DCS_P^{el} (M_f = 0)
10^{-16} cm^2/sr units
100
10
1
0.1
0.01
0
40
80
120
160
Angle (degree)

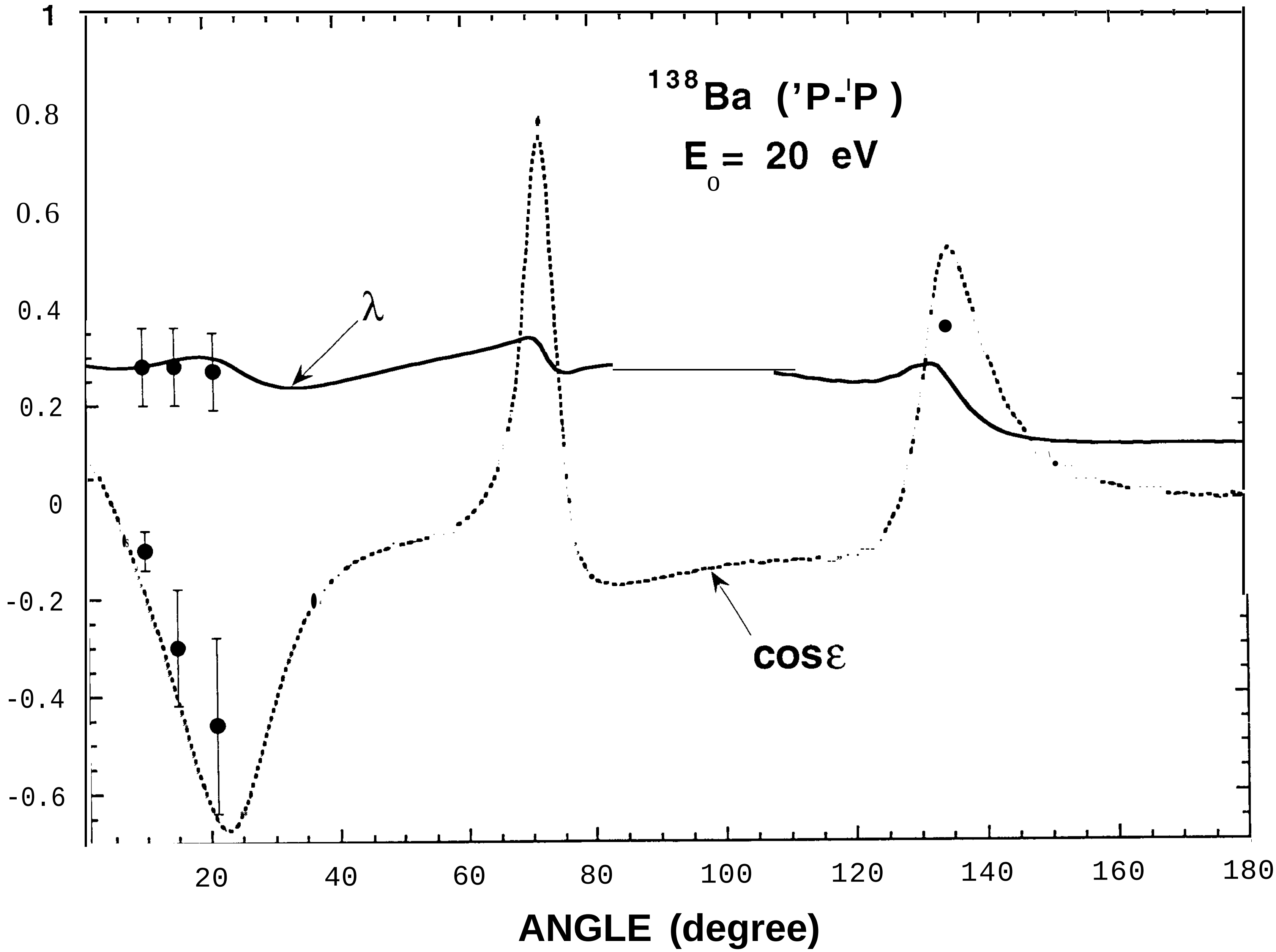
1
0.8
0.6
0.4
0.2
0
-0.2
-0.4
-0.6
^{138}Ba (^{1}P-^{1}P)
E_0 = 20 eV
λ
cosε
20
40
60
80
100
120
140
160
180
ANGLE (degree)